Swelling-induced structural changes and microparticle uptake of gelatin gels probed by NMR and CLSM

Carmine D'Agostino[(a)*†], Roberta Liuzzi[(b)†], Lynn F. Gladden[(a)], Stefano Guido[(b)(c)*]

[(a)] Department of Chemical Engineering and Biotechnology, University of Cambridge, Pembroke Street, Cambridge, CB2 3RA, UK

[(b)] Dipartimento di Ingegneria Chimica, dei Materiali e della Produzione Industriale, Università di Napoli Federico II, UdR INSTM, P.le Tecchio, 80, 80125, Napoli, Italy

[(c)] CEINGE Advanced Biotechnologies, via G. Salvatore 486, 80145 Napoli, Italy

*Corresponding Authors:

Dr Carmine D'Agostino

Department of Chemical Engineering and Biotechnology, University of Cambridge, Pembroke Street, Cambridge, CB2 3RA, UK, Email: cd419@cam.ac.uk, Tel: +44 (0)1223-334796

Prof Stefano Guido

Dipartimento di Ingegneria Chimica, dei materiali e della produzione industriale, Università di Napoli Federico II, P.le Tecchio, 80, 80125, Napoli, Italy, Email: steguido@unina.it, Tel: +39 081-7682271

† These two authors contributed equally to this work and are co-first authors.

Abstract

Gelatin gels are increasingly involved in many industrial applications due to several advantages including cost efficiency and biocompatibility. Generally, their production requires the use of aqueous solvents, which cause a significant swelling, due to the ability of solvent molecules to penetrate through the gel microstructure and increase its volume. Since swelling mechanisms and their effect on gel structure are not fully understood, further investigations are required. In this work, we combine macroscopic measurements of the swelling ratio (SR) with Nuclear Magnetic Resonance (NMR) and Confocal Laser Scanning Microscopy (CLSM) to investigate changes in gelatin structure as a function of both polymer concentration and swelling time. SR values increase as a function of time until a maximum is reached and then show a slight drop for all the gelatin concentrations after 24 h swelling time, probably due to a network relaxation process. NMR allows to determine mass transport and molecular dynamics of water inside the gelatin pores, while CLSM is used to visualize the penetration of tracers (polystyrene microbeads) with diameter much larger than the gel pores. Structural parameters, such as average pore size and tortuosity, are estimated. In particular, the pore size decreases for higher polymer concentration and increases during swelling, until reaching a maximum, and then dropping at longer times. The penetration of tracers provides evidence of the heterogeneity of the gel structure and shows that single microcarriers can be loaded in gelatin gels upon swelling.

Keywords: Gelatin gel, Swelling, Water mobility, Mesh size, NMR, Confocal Microscopy

INTRODUCTION

Gelatin is an animal protein derived from a partial hydrolysis of collagen, one of the main components of bones, skin, connective tissues and extracellular matrix. Based on the source[1] and on the pre-treatment of collagen, acid or alkaline, two different types of gelatin can be obtained, Type A and B, respectively. Although the amino acid composition is similar to that of the native collagen, the organization of the macromolecules (overlapping and cross-linked triple helices) is very different due to the manufacturing processes.[2, 3] At temperature above 40-50 °C gelatin is in a sol state while it forms an elastic gel by lowering the temperature below 30 °C, allowing a partial renaturing of collagen in a thermo-reversible manner. Moreover, factors such as humidity, initial gelatin concentration, temperature[4] and addition of cross-linkers can easily affect the final structure of the gelatin.[5]

Due to its versatility, gelatin is widely used in many applications including in the food industry,[6, 7] as ingredient or for confectionary, photographic, pharmaceutical and medical fields.[8] In the latter case, due to the biocompatibility and low costs, the use of gelatin is required not only as shell of hard or soft capsules, tablets and dietary supplements but also as scaffold for tissue engineering,[9, 10] for example as skin substitute[11] or cartilage regeneration.[12, 13] Despite the applications of gelatin are constantly increasing, there are still gaps in the full understanding of its structure and structure-related mechanisms.

Swelling of gelatin is one of the main processes responsible for its large use in industry. It has been demonstrated that this process depends on many factors, including temperature,[14] salt concentration in the solvent,[15] pH and charge distribution.[16] If cross-linkers are added,[17, 18] swelling is also affected by the cross-linker to gelatin mass ratio,[15, 19] thus resulting in a reduced water uptake, up to 50-60%, and a higher stiffness.[20] Swelling is determined by the ability of solvent molecules to intercalate between chains and disrupt inter-chains bonds forming hydrogen bonds with the amide groups of gelatin. This disruption allows the gel to swell, adsorbing a large amount of water. It has been noticed that the swelling rate of hydrogels is faster near the free edges compared to the centre of the gel.[21] When the equilibrium is reached, the excessive water is free to move in the large pores and between helices, which is also known as “free water” or “bulk water”.[22] Swelling kinetics is generally described with a second-order equation[16] controlled by diffusion of the solvent (water) and relaxation of the macromolecule chains.[23] However, all these studies have been focused on

the swelling equilibrium behaviour of chemically or physically cross-linked gel due to their higher stability.[24]

In understanding and rationalizing the macroscopic behaviour of gelatin, transport as well as structural properties of these systems, including pore size and pore network connectivity, are among the main aspects to consider, especially when gelatin is used as a medium for drug delivery. These parameters have been investigated by several techniques including electron microscopy imaging,[25, 26] dynamic light scattering or diffusion of labelled molecules of different sizes and molecular weights.[27] The former requires image analysis for pore size estimation, while in the latter diffusion of the labelled molecules is used as a marker to estimate pore dimensions and connection, based on the ability of the fluorescent marker to penetrate, together with the solvent, inside the gel.

Studies on gel samples by NMR have been so far focused on the determination of the gel point,[28] on cross-linked gel[29] or on the role of the solvent during gelation.[30] Different states of water have been identified in the gel. Water can be strongly entrapped in the helix becoming a structural part of the gel, thus its mobility is very slow; it can locate between helices whose movement is faster; or it can be significantly far from the interface of the network such that is not affected by it, therefore retaining the molecular dynamics of free bulk water.[31] Discrepancies on the real existence of all these states in the gel are still a matter of debate, each case being dependent on the specific conditions. Therefore, a complete overview on alteration of the gelatin structure following different mechanisms is still lacking.

In this work, NMR is presented as non-invasive, powerful technique to study molecular dynamics of water inside gelatin structures. In particular, we use spin-lattice relaxation measurements, T_1, and pulsed-field gradient (PFG) NMR diffusion measurements to probe rotational and translation dynamics of water confined in gelatin structures, studying the effect of different parameters, most notably, polymer concentration and swelling time. In addition, possible changes in the gelatin structure due to diffusion of polystyrene particles of different dimensions are also investigated by both NMR and CLSM. Self-diffusion coefficient of water, average pore size and tortuosity of the porous matrix for all the samples are also estimated.

MATERIALS AND METHODS

Materials

Type A gelatin was available commercially by Extraco Gelatin under the trade name of Geltec (UG-719- H) derived from collagenous tissue by acid treatment and supplied in powder form. The molar mass of the gelatin is 1.4×10^5 g mol^{-1}.

Mineral oil was purchased from Sigma-Aldrich. Polystyrene particles with diameter of 0.1 μm and 1 μm were supplied, respectively, by Sigma-Aldrich and Bangs Laboratories Inc. Particle solutions were obtained by suspending particles in aqueous buffer at a solid concentration of 1%. For CLSM experiments, fluorescent polystyrene particles of 0.1 μm (Polyscience) and 1 μm (Sigma-Aldrich) were prepared in suspension as in the previous case.

Methods

Gelatin solution preparation

Gelatin solutions at concentrations of 10, 15, 20 and 30% by weight were obtained by dissolving a proper amount of gelatin powder in distilled water under gentle stirring for 1 h at 60 °C until a homogeneous solution was obtained.

Swelling measurements

Gelatin solutions obtained as previously described were injected in a glass mold (25×15×1mm) and cooled slowly at room temperature until complete gelation. Since the gelation time depends on the polymer concentration, a conservative gelation time of approximately 1 h was used for all the samples. Specimens were collected from the mold, transferred, soaked, and maintained at room temperature (about 25 °C) in different aqueous buffer solutions until equilibrium was achieved. A thin layer of mineral oil was applied at the bottom of the reservoir in order to avoid gel sticking. Permeability of mineral oil in water is very low and its use is advised when water loss from hydrogel has to be minimized.[21] Swelling was measured gravimetrically. At different time intervals, samples were collected from the aqueous buffer solutions and weighed. Excess solvent was removed gently with a filter paper. The total length of the experiments was 72 h. The swelling ratio was estimated according to the following equation:

$$SR\% = \left(\frac{W_t - W_0}{W_0}\right) \times 100 \quad (1)$$

where W_t is the weight of the swollen gel at time t and W_0 is the initial weight of the sample.

Effect of polymer concentration and swelling time probed by NMR

For NMR measurements of gelatin at different polymer concentrations, in the range 10-30% by weight, gelatin solutions were directly injected in the NMR tube (4 mm) and allowed to gel, avoiding formation of air bubbles. Gels were directly prepared in the NMR tubes also to avoid possible breaking or alteration of the structure during the insertion in the tube. For the investigation of the swelling effect, gelatin at 30% by weight was allowed to gel and then small cylinder punches with 2 mm diameter and 3 cm length, were allowed to swell in aqueous solution and were then collected after 2, 5, 18, 24, 48 and 72 h before being gently inserted into the NMR tubes.

Effect of solid particle penetration probed by NMR

Gelatin at 30% by weight was prepared directly into the NMR tubes as previously described. After gelation, 200 µL of polystyrene particle solution at 1% was added on the top of the gel and samples were then sealed and kept at room temperature for 24 h. After this time, part of the solution was adsorbed by the sample due to the swelling, while excessive solution was removed and the sample analyzed by NMR.

Effect of solid particle penetration probed by CLSM

For CLSM experiments, gelatin at 30% by weight was prepared directly in a Ibidi µ-slide multi-well (9.4×10.7×6.8 mm) and allowed to gel. After gelation, half of the sample was removed with the aid of a knife and the empty zone replaced with fluorescent particle solutions. Samples were kept sealed in order to prevent water evaporation from the solution and drying of the gel. For the first two hours a time lapse was acquired in brightfield by an inverted Leica TCS SP5 CLSM equipped with an Ar laser and a 20× objective starting from the interface between the gel and the solution in order to follow the swelling of the interface. The delay time between acquisitions was of 1 min. After 24 h samples were analyzed in order to investigate the ability of particles of different dimensions to penetrate the gel network and assess possible changes in the gel structure. Images were acquired with a 63× oil immersion objective along the entire gel sample and the maximum distance reached by particles was estimated. The density of particles was measured by dividing the number of particles by the image area in μm^2. This operation was repeated for 11 images at different depths in the

sample and the mean density was estimated. Image analysis was carried out using the commercial software Image Pro Plus 6.0. Results about the ability of particles to penetrate the gel were then compared with NMR results on water diffusion and relaxation properties within the gel in the presence of particles.

NMR experiments

All the NMR experiments were performed at room temperature on a Bruker Biospin DMX 300 operating at a ^{1}H frequency of 300.13 MHz using a Bruker Biospin Diff-30 diffusion probe capable of producing magnetic field gradient pulses up to 11.76 T m^{-1}. NMR T_1 relaxation times were measured using the standard inversion recovery pulse sequence.[32] The T_1 relaxation time constant was obtained by fitting the experimental data on the NMR signal intensity as a function of the time delay, $S(t)$, to the equation:[32]

$$S(t) = S_0\left[1 - 2\exp\left(-\frac{t}{T_1}\right)\right] \quad (2)$$

^{1}H PFG NMR diffusion measurements were performed using the alternating pulsed gradient stimulated echo (APGSTE) sequence[33] in order to minimize the effects of background magnetic field gradients. The measurements were carried out holding the gradient pulse duration, δ, constant and varying the magnetic field gradient strength, g. The gradient pulse duration, δ, was set to 1 ms. For each sample, the observation time, Δ, was varied from 20 to 1600 ms and no significant differences in the PFG log attenuation plots were observed, which implies that the self-diffusion coefficient of water inside the porous gelatin is essentially independent of the observation time (see Supplementary Information S1). Values of the diffusion coefficient, D, were obtained by fitting the PFG NMR experimental data to the expression:[34]

$$\frac{E(g)}{E_0} = \exp\left[-D\gamma^2 g^2 \delta^2 (\Delta - \delta/3)\right] \quad (3)$$

where $E(g)$ and E_0 are the NMR echo signal intensity in the presence and absence of magnetic field gradient, respectively.

RESULTS AND DISCUSSION

Swelling ratio

The swelling ratio (SR), quantified using Equation (1), as a function of time for gel samples at concentrations ranging from 10 to 30%, is reported in Figure 1. The results indicate an increase of adsorbed water for gels with lower polymer concentration. Initially, all trends overlap, showing a fast swelling rate. After 2 h, the trends show a lower swelling rate and start to differentiate from each other, until reaching an equilibrium state. Samples at 20% and 30% polymer concentration show a similar trend, with a slight difference around 48 h, where the 20% gel shows a slightly lower SR. It is worth mentioning that for all samples, at longer time the equilibrium value tends to drop slightly. Although such a drop is not large, it is observed in all cases. This result could suggest that the excessive water in the sample leads to a slight weakness of the network. This effect is more pronounced for the 10% gel, which starts to drop after already 24 h, while the other samples generally show a similar behaviour after a longer swelling time. This can be explained by the higher amount of the polymer, which guarantees a higher stability and starts to relax at longer times.[35]

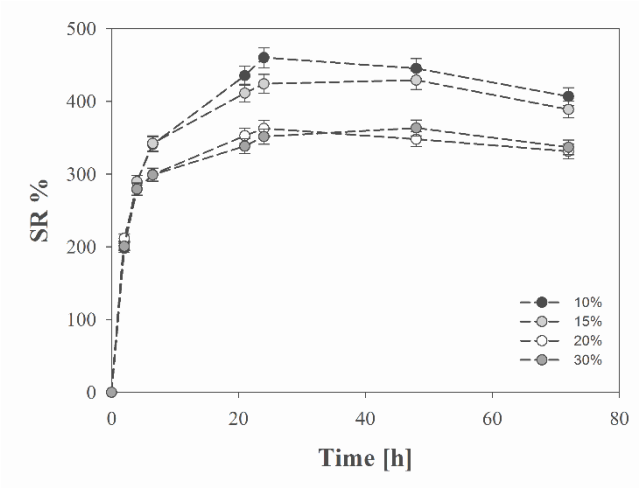

Figure 1. Swelling ratio of gelatin samples at 10%, 15%, 20% and 30% by weight polymer concentration.

Effect of gelatin concentration

Figure 2 shows typical T_1 inversion recovery (Figure 2a) and PFG diffusion log attenuation plots (Figure 2b) of water within the gelatin structure at different polymer concentrations. Plots for the other samples are of similar quality. The plots in Figure 2 clearly show significant changes of relaxation and diffusion properties of water as the polymer concentration increases. By inspection of the plots, it is already possible to see as, relatively

to water confined within the gelatin structures, bulk water has a significantly longer T_1, i.e., slower recovery of magnetization in Figure 2a, and a higher self-diffusion coefficient, i.e., a steeper slope in Figure 2b. As the polymer concentration increases, the T_1 of water becomes shorter and its self-diffusion coefficient slower, which indicates a slowing down of molecular dynamics due to the confinement within the gelatin pore structure.

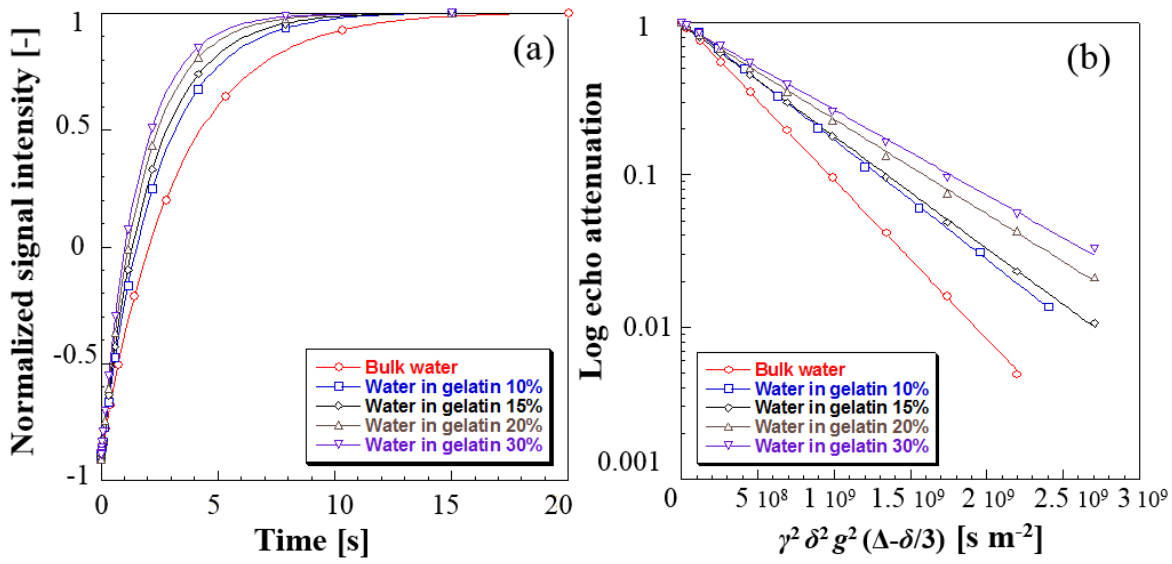

Figure 2. (a) T_1 inversion recovery and (b) PFG log attenuation plots of water in gelatin at different polymer concentration. Solid lines are fitting to: (a) Equation (2) and (b) Equation (3).

From the data in Figure 2, using Equations (2) and (3), it is possible to evaluate the values of the T_1 relaxation time and self-diffusion coefficient, D, of water as a function of polymer concentration, which are reported in Figure 3.

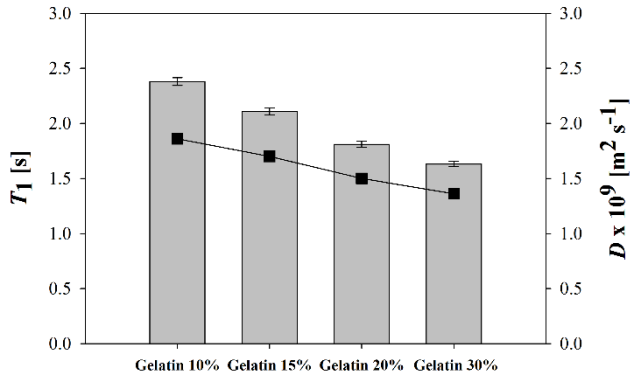

Figure 3. T_1 relaxation time (columns) and self-diffusion coefficient D (squares) of water inside gelatin with different polymer concentration. For free bulk water T_1 = 3.22 s and D = 2.35×10^{-9} m^2 s^{-1}. The solid line is a guide to the eye.

It is clear that as the percentage of polymer increases, both the T_1 and D values decrease, which is consistent with a reduced rotational and translational dynamics[36] of water molecules as the polymer concentration increases. In particular, the observed T_1 relaxation rate can be written as:[37]

$$\frac{1}{T_1} = \frac{1}{T_{1,\text{bulk}}} + \frac{S}{V}\rho_1 \tag{4}$$

where $1/T_{1,\text{bulk}}$ is the relaxation rate of the bulk fluid and, once the temperature is fixed, this is a constant, ρ_1 is the surface relaxivity, which is a property of the material and for the system under investigation can be assumed to be constant across the samples, and S/V is the surface-to-volume ratio of the gelatin structure. Therefore, a decrease in T_1, that is, an increase of the $1/T_1$ relaxation rate, implies an increase of S/V.

In order to further investigate the diffusive behaviour of water inside the gelatin structure, PFG NMR experiments were carried for a range of different observation times, Δ, and the results are reported in Table 1.

Table 1. Self-diffusion coefficient, *D*, of water for gelatin with different polymer concentration as a function of the observation time, Δ.

	Self-diffusion coefficient, *D*, [m^2 s^{-1}] × 10^9			
	Δ = 20 ms	**Δ = 200 ms**	**Δ = 800 ms**	**Δ = 1600 ms**
Gelatin 10%	1.89 ± 0.05	1.86 ± 0.05	1.83 ± 0.05	1.87 ± 0.05
Gelatin 15%	1.74 ± 0.04	1.70 ± 0.04	1.70 ± 0.04	1.71 ± 0.04
Gelatin 20%	1.54 ± 0.04	1.50 ± 0.04	1.47 ± 0.04	1.48 ± 0.04
Gelatin 30%	1.40 ± 0.04	1.36 ± 0.03	1.35 ± 0.03	1.34 ± 0.03

The results in Table 1 clearly show that the self-diffusion coefficient of water in the gelatin samples is lower than that of bulk water, 2.35×10^{-9} m^2 s^{-1}, and is essentially independent of the observation time. This result, together with the lack of curvature of the PFG plots (Figure 2b) implies that already at 20 ms water molecules are probing regions of the pore space that are representative of the whole porous structure. Indeed, the root mean square displacement,

$RMSD = \sqrt{2D\Delta}$, calculated at 20 ms is already of the order of tens of μm, which is far greater than the typical pore size for these gelatin systems, which of the order of tens of nm.[38] Hence, within the probed observation time, molecules experience many collisions with the pore walls and their diffusion is reduced by the presence of the pore network.[36] This behaviour is typical of mesoporous systems with a macroscopically homogeneous pore structure and is referred to as *quasi-homogeneous* behaviour.[36, 39] For the following analysis, values of *D* at 200 ms were considered.

In order to obtain more insights into the effect of polymer concentration on the pore network properties, we define the following parameters:[36]

$$\eta = \frac{T_{1,\text{bulk}}}{T_{1,\text{pore}}} \tag{5}$$

$$\xi = \frac{D_{\text{bulk}}}{D_{\text{pore}}} \tag{6}$$

In the above expressions, the subscript "bulk" indicates free bulk water whereas the subscript "pore" indicates water confined within the gelatin pore network. The η parameter may be considered as an indication of the extent to which rotational dynamics of molecules within the pore network is reduced relative to the bulk.[36] The parameter ξ is the so-called PFG interaction parameter,[36, 40] which indicates the extent to which translational dynamics of molecules within the pore network is reduced relative to the bulk and can be considered a measure of the apparent tortuosity of the porous media, that is, the tortuosity experienced by water molecules diffusing within the pore network. Both parameters have been previously used to understand and explain changes in molecular dynamics of various fluids in different porous materials.[36] For fluids in pores behaving as bulk fluids both parameters are equal to one; an increase of such parameters inside pore structures indicates a slower molecular dynamics. The values of these parameters for water within the gelatin samples under investigation in this work are reported in Figure 4.

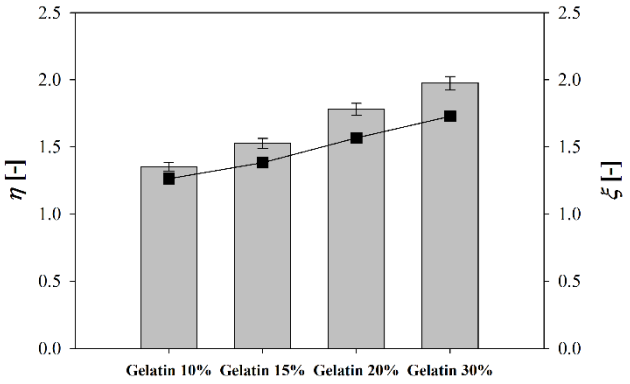

Figure 4. Values of η (columns) and ξ (squares) parameters of water in gelatin with different polymer concentration. For water behaving as free bulk water η and ξ are equal to one. The solid line is a guide to the eye.

From Figure 4 two important conclusions can be drawn: *(i)* the increase in polymer concentration reduces the rotational dynamics of water inside the gelatin relative to the bulk fluid, indicating an increase in porosity and surface-to-volume ratio, *S*/*V*, of the pore structure, which could be due either to an increase of contact surface area of water with the gelatin, due to the increase of polymer amount, but also to a reduction of pore size as the polymer concentration increases; *(ii)* at the same time, the increase in polymer concentration is changing the pore network connectivity, with a more tortuous pore structure at higher polymer concentrations, that is, higher values of ξ.

Effect of swelling time

It is now interesting to analyze the effect of swelling time over the molecular dynamics of water inside the porous gelatin structure and on the properties of the pore structure itself. These results are reported in Figure 5.

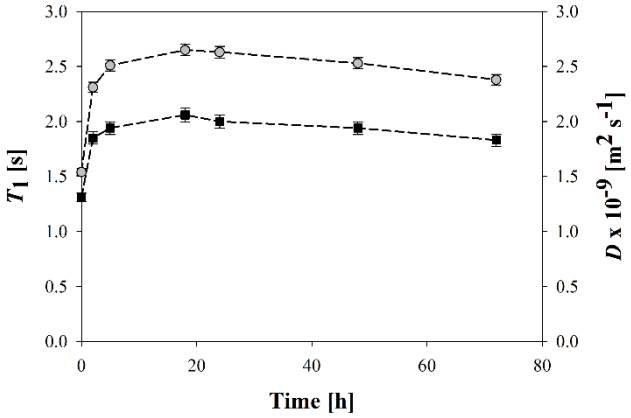

Figure 5. T_1 relaxation time (circles) and self-diffusion coefficient D (squares) of water in gelatin 30% sample as a function of the swelling time.

From Figure 5 it is possible to observe that both T_1 and D increase rapidly in the first 5 h of swelling. Such values reach an apparent plateau but then experience a slight decrease at longer times, with values at 72 h swelling being lower that those recorded in the range 20-40 h. This behaviour is similar to that of the SR as a function of time, reported in Figure 1 and strongly suggests a link between the NMR measured quantities and the macroscopic measured SR. The changes in T_1 and D imply that the swelling time is having two main effects on the pore structure. Firstly, the increase in T_1 clearly suggests that as the swelling proceeds, the rotational dynamics of water inside the pore becomes closer to that of bulk water, the latter having a value of T_1 = 3.22 s. Given that in this case the polymer concentration is the same, this effect can be explained by an increase in the average pore size, with a consequent decrease of S/V, as suggested by Equation (4). This implies that the effect of the gelatin surface (i.e., surface relaxivity) on water molecular dynamics decreases and the fluid behaves more like the free bulk fluid. In addition, the increase in swelling time is also increasing the diffusion coefficient of water inside the pore structure, which, analogously to the T_1 behaviour, becomes closer to the self-diffusion coefficient of free bulk water, the latter having a value of 2.35×10^{9} m^2 s^{-1}. These findings are in good agreement with what has been previously suggested when studying swelling of hydrogel.[22, 41] The values of the η and ξ parameters for gelatin samples at different swelling times are reported in Figure 6.

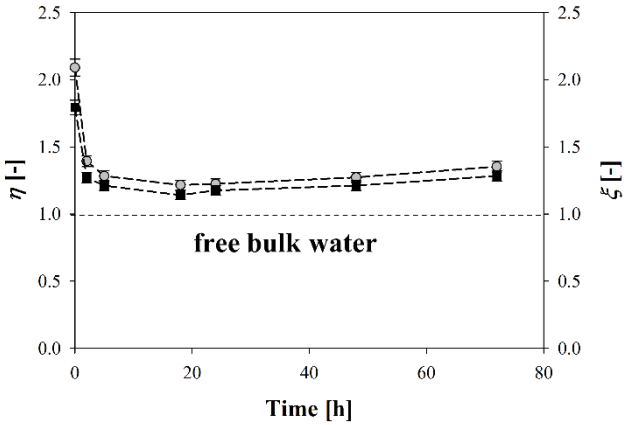

Figure 6. Values of η (circles) and ξ (squares) parameters of water in gelatin 30% sample as a function of swelling time. For water behaving as free bulk water η and ξ are equal to one (black dotted line).

From Figure 6 it is possible to observe that as the swelling time increases the value of η starts to decrease approaching one, which implies that the rotational dynamics of water inside the porous gel becomes closer to that of free bulk water. As previously explained, this can be attributed to an enlargement of the pore structure and consequent increase of the average pore size. The trend for the apparent tortuosity, ξ, is very similar to that observed for η, which implies that the swelling of the porous matrix improves pore network connectivity and hence improving water mass transfer by diffusion. However, at longer time such values start experiencing a slight increase. The increase in such values is subtle but significant and is observed for both parameters and could be attributed to a shrinking of the pore network due to a possible relaxation of the structure. This is indeed supported by the results on the SR shown in Figure 1, which indeed suggest a slight relaxation at a macroscopic level of the pore structure after the initial swelling. This finding is significant because it highlights a link between changes in microscopic properties of the gelatin, probed using NMR methods, and macroscopic changes in the SR with time. It is important to point out that in order to confirm the results reported in Figures 5 and 6, NMR measurements of T_1 and D were repeated several times, using the same samples but also with different batches. The results and the trend were consistent and confirmed in all cases.

Polystyrene particle permeation experiments

Penetration of fluorescent polystyrene particles of two different dimensions, 0.1 µm and 1 µm diameter, in a 30% gelatin gel were used as models to investigate possible changes in the gel structure. A similar approach can be useful to mimic the behaviour of polymeric particles when used as carriers for active principles during drug-loaded gels and delivery,[42] the latter dependent on the degree and rate of swelling as well as on gelatin concentration and gelatin-particles interaction. A schematic representation of our setup and results are reported in Figure 7. Firstly, the swelling of the gel interface was recorded during a 2 h time lapse with a delay time of 1 min (Figure 7a). It is possible to observe that the gel interface slides quickly according with the results in Figure 1, where the first 2 hours show a higher swelling rate. All other faces of the sample are immobilized by the walls and therefore cannot swell except for the upper face in contact with air, which is free to swell. However, due to the experimental conditions, where water does not cover the gel sample, but it is in contact with it only on the lateral side, this effect, if any, is negligible. It is well known, indeed, that the SR depends on the conditions and the effective free surface in contact with water.[43] The SR of the interface, estimated by measuring initial and final length of the gel is around 7% in 2 h. It was not possible to carry out a continuous time lapse for 24 h as the gel interface exceeded the field of view. However, it was possible to estimate a 24 h SR of the interface of approximately 20%. Obviously, this value of SR has not to be compared with SR reported above in Figure 1 because in this case the SR is related only to one face of the sample, which is in direct contact with the solvent.

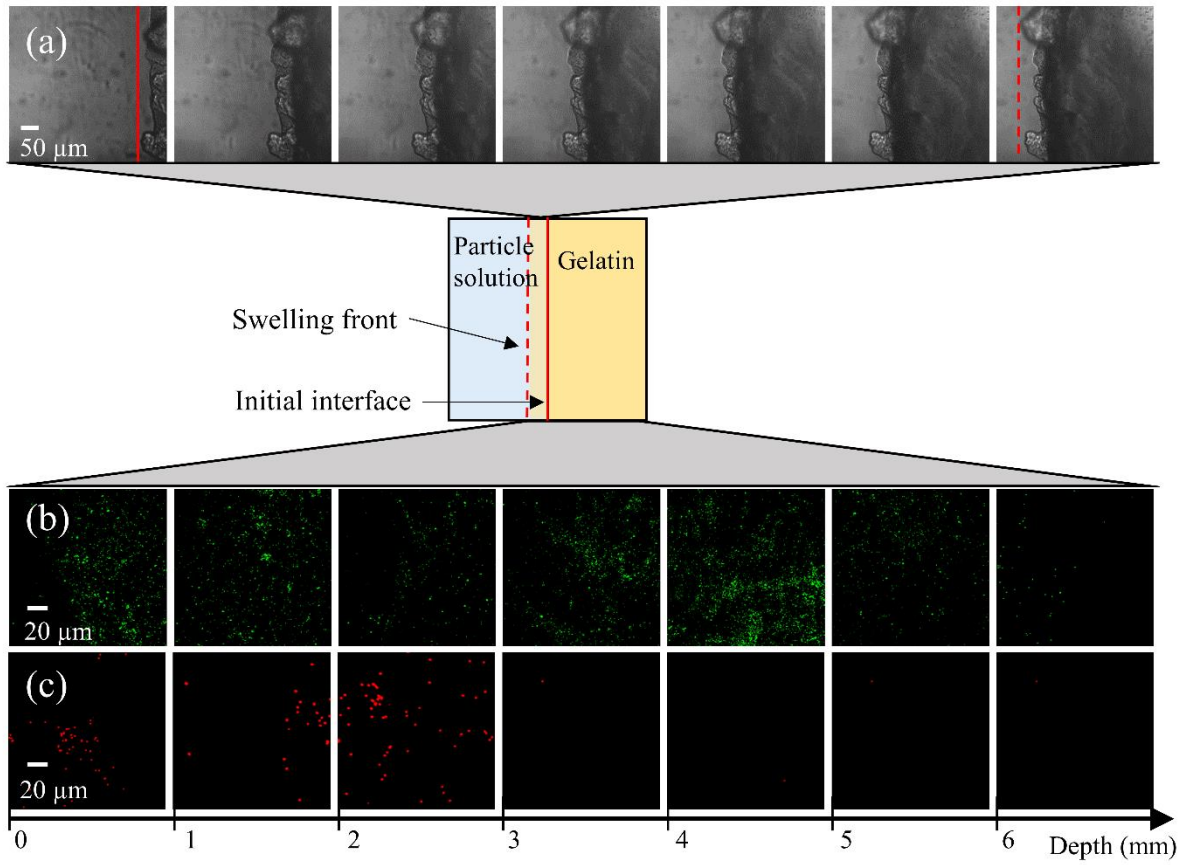

Figure 7. Schematic representation of the setup for permeation experiments of polystyrene particles. (a) Swelling of the gel interface during 2h time lapse. Solid and dotted red lines represent respectively, the initial interface and the swelling front of the gelatin gel. Diffusion of 0.1 µm (b) and 1 µm (c) polystyrene particles in the gel after 24 h.

Regarding particle permeation, even if not fully appreciable from the images, the time lapse shows that during the first two hours, particles do not start immediately to penetrate the gel but it seems that due to the swelling, corresponding to a net displacement of the interface, the latter is able to push particles in the swelling direction retarding their entrance. After 24 h, however, it is possible to reconstruct the whole path of the particles inside the gel. Parts of this path, reported in Figure 7b-c show that both particles penetrate the gel. Whilst 0.1 µm particles diffuse through the entire sample reaching the second interface at a distance of about 6 mm, 1 µm particles stop their run shortly after passing the interface. The distribution of both particles in the gel is not uniform and the mean density is also significantly different, with values of 0.04 and 0.01 for 0.1 µm and 1 µm particles, respectively, suggesting that 1 µm particles diffuse but they are more affected by the network hindrance. The limited particle penetration can be explained by considering that the distribution of pore dimension can be

highly heterogeneous. Considering also the further increase in mesh size due to swelling, it is likely that both particles, even if with dimensions much larger than the average gelatin pores, can find sufficiently large pores to pass through. Moreover, at least during swelling, it is possible that the convective transport of the particles in water creates a stress concentration around them, which can lead to further changes in network microstructure. These results, together with the NMR experiments reported in the following section, suggest a new method to improve drug-loading of gelatin gels used for drug delivery. In fact, one of the main problems faced during drug-carriers encapsulation in gelatin gels is the formation of aggregates, which strongly influence drug stability and release. The images of Figure 7, on the contrary, show that particles, although distributed in a non-uniform manner, do not tend to aggregate in clusters.

Effect of polystyrene particles on the gelatin structure

In order to understand the effect of particle penetration on the pore structure of the gel, T_1 and PFG NMR diffusion experiments were carried out on gelatin 30% samples in contact with aqueous suspensions of polystyrene particles of 0.1 and 1μm. The results for T_1 relaxation times and self-diffusion coefficients, D, of water and the corresponding η and ξ parameters for these samples are reported in Figure 8.

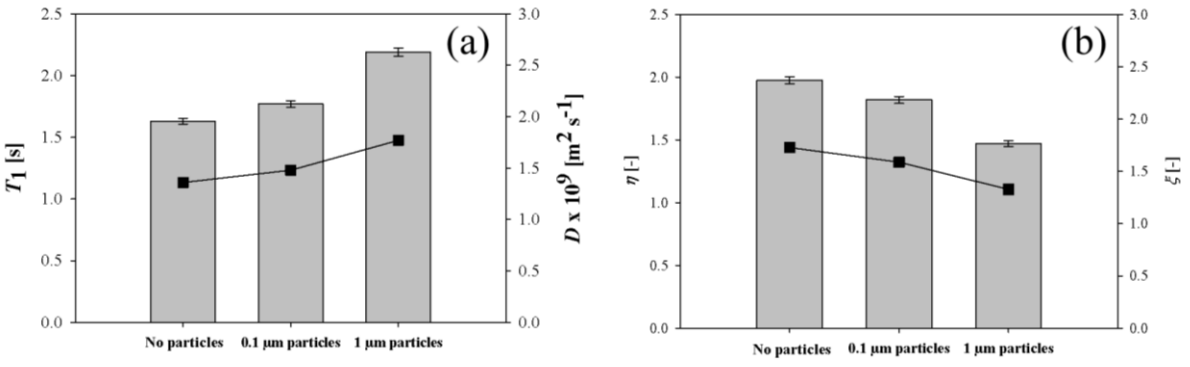

Figure 8. (a) Effect of solid particles on T_1 relaxation time (columns) and self-diffusion coefficient D (squares) of water in gelatin 30% sample. (b) Effect of solid particles on η (columns) and ξ (squares) parameters of water in gelatin 30%. For water behaving as free bulk water η and ξ are equal to one.

Figure 8a shows that the penetration of solid particles inside the gel is modifying the T_1 relaxation time and self-diffusion coefficient of water. In particular, larger particles contribute to an increase of both properties with a consequent decrease of η and ξ (Figure 8b), which become closer to the value of one for free bulk water. It is possible that the penetration of solid particles inside the gel occurs through larger pores, which result in the observed increase for T_1, and at same time improves the pore network connectivity, hence enhancing diffusion within the pore network. It is reasonable that larger particles tend to cause more significant changes in pore structure and indeed, this is in line with the results reported in Figure 8.

Estimation of average pore size

Using the expression in Equation (4) and assuming the pores to be of cylindrical geometry, the observed T_1 relaxation rate can be written as:

$$\frac{1}{T_1} = \frac{1}{T_{1,\text{bulk}}} + \frac{4}{d}\rho_1 \qquad (7)$$

where d is the average pore diameter. Therefore, if the surface relaxivity ρ_1 is known, it becomes possible to calculate the average pore size of the porous gel from the observed $1/T_1$ relaxation rate values. The surface relaxivity can be estimated from Equation (7) using the value of observed T_1 relaxation rate measured for the 10% gelatin sample and using the average pore diameter of 20 nm reported in the literature for this sample,[38] which gives $\rho_1 \approx 5.5x10^{-4}$ μm s^{-1}. This value of surface relaxivity is significantly smaller than those reported in the literature for solid porous materials such as sandstones and other porous oxides[44, 45] and this is largely expected given the absence of strong relaxation sinks such as paramagnetic ions and strong adsorption sites, which are typical of porous materials such as concrete, rocks and catalysts.[45-47] Once the surface relaxivity of the gelatin is estimated, it becomes possible to estimate the average pore size for the different samples using Equation (7). The values are reported in Figure 9 as a function of polymer concentration (Figure 9a) and for the gelatin

30% sample as a function of the swelling time (Figure 9b). The range for the calculated average pore diameter is in good agreement with the average pore size reported for these systems, which ranges from tens of nm down to a few nm. [48-52]

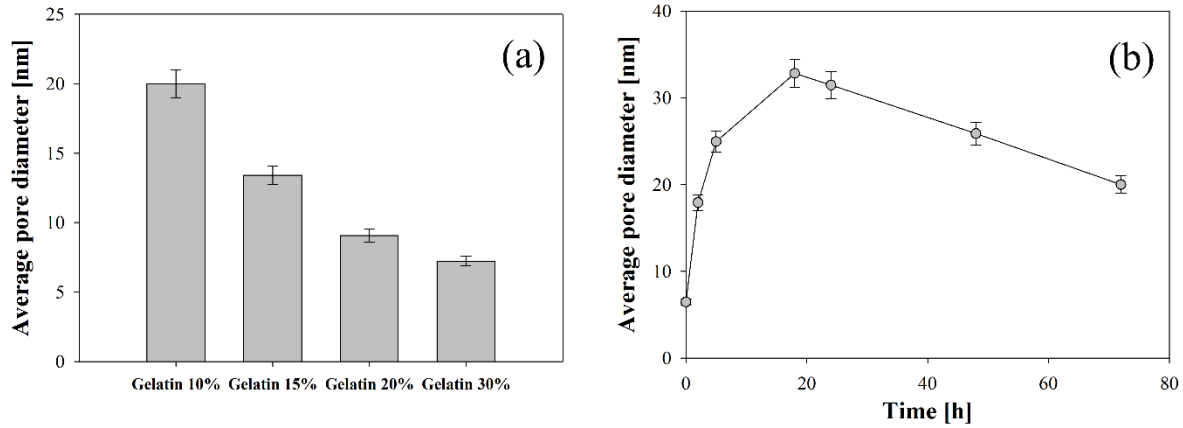

Figure 9. Average pore diameter calculated using Equation (7) for: (a) samples at different polymer concentration; (b) gelatin 30% sample as a function of the swelling time.

From Figure 9a it is possible to observe that as the polymer concentration is increased, the average pore size decreases to approximately 7 nm for the gelatin 30% samples. Figure 9b shows that the average pore diameter of the gelatin 30% sample increases more sharply in the first 5 hours of swelling, it then reaches a maximum at approximately 24 h, with an average pore size of approximately 32 nm, and then decreases reaching a value of approximately 20 nm at 72 h. This behaviour is very similar to that observed for the swelling ratio, SR, and it suggests that SR and average pore diameter are closely related. Indeed, it is interesting to note that this behaviour is consistent with the trend observed for the swelling ratio, Figure 1, which also reaches a plateau but then undergoes a slight decrease at longer times. The similarity between these independent findings support the idea that the gelatin structure after an initial expansion may undergo some sort of relaxation of the pore structure, which results in a shrinkage with a consequent decrease of pore size.

CONCLUSIONS

In this work, NMR and CLSM are presented as insightful tools to investigate gelatin gel structures. The influence of the initial polymer concentration and swelling times are assessed. Firstly, the swelling ratio, SR, has been measured for four different gelatin samples in the

concentration range 10% - 30% (wt/wt) of gelatin. Results have shown that water uptake and corresponding SR is higher in the case of lower concentrations of gelatin. Moreover, it was interesting to note a slight weakness of the gelatin structure after equilibrium was reached, probably due to a starting relaxation of the network. NMR experiments have confirmed significant changes of relaxation and diffusion properties of water molecules as the polymer concentration increases. In particular, from the decrease in the T_1 relaxation time of the fluid confined within the gelatin structure, due to an increase in polymer concentration, it is possible to observe an increase in surface-to-volume ratio of the pore structure, which is attributed to a reduction of the average pore dimension. Moreover, from NMR self-diffusion coefficients, *D*, it is possible to infer that the increase in polymer concentration causes also an increase of the tortuosity of the pore network. The effect of swelling time was also assessed. The initial rapid increase of both, T_1 and *D* of water as a function of the swelling time suggests that water mobility is approaching that of the free bulk water, which is due to an increase in pore size and an improved pore network connectivity, i.e., decrease in tortuosity, and consequent enhancement of water mass transport by diffusion. However, at longer times both T_1 and *D* values experience a slight but appreciable decrease which, in conjunction with the results on SR measurements, suggests that the gelatin structure is experiencing a slight shrinkage after a rapid initial expansion.

Further alterations of the gelatin structure have been demonstrated by analysing samples after penetration of polystyrene particles of 0.1 and 1 μm diameter. Results have shown that both particles penetrate the gel structure, with the larger particles, in turn, affecting more the gelatin pore network and improving pore network connectivity. The limited number of pores larger than 1 μm explains the lower mean concentration of 1 μm particles compared to 0.1 μm particles. These results have been also supported by CLSM visualization, showing that 1 μm particles are able to slowly intercalate in the network, although they stop their permeation at a short distance from the interface. Finally, the average pore size, using T_1 relaxation measurements, has been estimated in the range 7-21 nm for gelatin concentrations in the range 10%- 30%. The change in pore size of the 30% gelatin sample with swelling time was also estimated.

In conclusion, a combination of NMR and CLSM can reveal new insights into molecular dynamics and microsctructure of gelatin and how this is affected by various parameters, including polymer composition, swelling ratio as well as the penetration of solid particles. Such knowledge is of importance for applications in many fields such as using gelatin as a drug-loading gel.

Acknowledgements

Carmine D'Agostino would like to acknowledge Wolfson College, Cambridge, for supporting his work and activities. Roberta Liuzzi would like to acknowledge Prof. Pietro Cicuta for the opportunity to stay at University of Cambridge and collaborate for this work.

References

1. M. Gómez-Guillén, J. Turnay, M. Fernández-Dıaz, N. Ulmo, M. Lizarbe and P. Montero, *Food Hydrocolloids*, 2002, **16**, 25-34.
2. L. Ghasemi-Mobarakeh, M. P. Prabhakaran, M. Morshed, M.-H. Nasr-Esfahani and S. Ramakrishna, *Biomaterials*, 2008, **29**, 4532-4539.
3. S. Caserta, L. Sabetta, M. Simeone and S. Guido, *Chemical engineering science*, 2005, **60**, 1019-1027.
4. S. M. Tosh, A. G. Marangoni, F. R. Hallett and I. J. Britt, *Food Hydrocolloids*, 2003, **17**, 503-513.
5. A. Duconseille, T. Astruc, N. Quintana, F. Meersman and V. Sante-Lhoutellier, *Food Hydrocolloids*, 2015, **43**, 360-376.
6. A. Karim and R. Bhat, *Trends in food science & technology*, 2008, **19**, 644-656.
7. A. Karim and R. Bhat, *Food hydrocolloids*, 2009, **23**, 563-576.
8. K. B. Djagny, Z. Wang and S. Xu, *Critical reviews in food science and nutrition*, 2001, **41**, 481-492.
9. S. Van Vlierberghe, P. Dubruel and E. Schacht, *Biomacromolecules*, 2011, **12**, 1387-1408.
10. B. V. Slaughter, S. S. Khurshid, O. Z. Fisher, A. Khademhosseini and N. A. Peppas, *Advanced materials*, 2009, **21**, 3307-3329.
11. E. Chong, T. Phan, I. Lim, Y. Zhang, B. Bay, S. Ramakrishna and C. Lim, *Acta biomaterialia*, 2007, **3**, 321-330.
12. T. Guo, J. Zhao, J. Chang, Z. Ding, H. Hong, J. Chen and J. Zhang, *Biomaterials*, 2006, **27**, 1095-1103.
13. S.-M. Lien, L.-Y. Ko and T.-J. Huang, *Acta Biomaterialia*, 2009, **5**, 670-679.
14. S. E. Kudaibergenov and V. B. Sigitov, *Langmuir*, 1999, **15**, 4230-4235.
15. C. H. Lee and Y. C. Bae, *Macromolecules*, 2015, **48**, 4063-4072.
16. C. Qiao and X. Cao, *Journal of Macromolecular Science, Part B*, 2014, **53**, 1609-1620.
17. M. Azami, M. Rabiee and F. Moztarzadeh, *Polymer Composites*, 2010, **31**, 2112-2120.
18. S.-M. Lien, W.-T. Li and T.-J. Huang, *Materials Science and Engineering: C*, 2008, **28**, 36-43.
19. Q. Xing, K. Yates, C. Vogt, Z. Qian, M. C. Frost and F. Zhao, *Scientific reports*, 2014, **4**.
20. X. Lou and T. V. Chirila, *Journal of biomaterials applications*, 1999, **14**, 184-191.
21. R. H. Pritchard and E. M. Terentjev, *Polymer*, 2013, **54**, 6954-6960.
22. A. S. Hoffman, *Advanced drug delivery reviews*, 2012, **64**, 18-23.

23. H. Schott, *Journal of Macromolecular Science, Part B: Physics*, 1992, **31**, 1-9.
24. M. Gómez-Guillén, B. Giménez, M. a. López-Caballero and M. Montero, *Food Hydrocolloids*, 2011, **25**, 1813-1827.
25. X. Liu and P. X. Ma, *Biomaterials*, 2009, **30**, 4094-4103.
26. H.-W. Kang, Y. Tabata and Y. Ikada, *Biomaterials*, 1999, **20**, 1339-1344.
27. L. C. Dong, A. S. Hoffman and Q. Yan, *Journal of Biomaterials Science, Polymer Edition*, 1994, **5**, 473-484.
28. T. Brand, S. Richter and S. Berger, *The Journal of Physical Chemistry B*, 2006, **110**, 15853-15857.
29. R. Dash, M. Foston and A. J. Ragauskas, *Carbohydrate polymers*, 2013, **91**, 638-645.
30. J. Maquet, H. Theveneau, M. Djabourov, J. Leblond and P. Papon, *Polymer*, 1986, **27**, 1103-1110.
31. P. Belton, *International journal of biological macromolecules*, 1997, **21**, 81-88.
32. E. Fukushima, Roeder, S.W., *Experimental pulse NMR*, Addison-Weslkey, Reading, US, 1981.
33. R. M. Cotts, M. J. R. Hoch, T. Sun and J. T. Markert, *Journal of Magnetic Resonance*, 1989, **83**, 252-266.
34. J. E. Tanner, *Journal of Chemical Physics*, 1970, **52**, 2523-2526.
35. D. Biswal, B. Anupriya, K. Uvanesh, A. Anis, I. Banerjee and K. Pal, *Journal of the mechanical behavior of biomedical materials*, 2016, **53**, 174-186.
36. C. D'Agostino, J. Mitchell, L. F. Gladden and M. D. Mantle, *The Journal of Physical Chemistry C*, 2012, **116**, 8975-8982.
37. P. J. Barrie, *Annual Reports on NMR Spectroscopy*, 2000, **41**, 265-316.
38. S. Ma, M. Natoli, X. Liu, M. P. Neubauer, F. M. Watt, A. Fery and W. T. Huck, *Journal of Materials Chemistry B*, 2013, **1**, 5128-5136.
39. M. Dvoyashkin, R. Valiullin and J. Kärger, *Physical Review* 2007, **75**, 041202.
40. M. D. Mantle, D. I. Enache, E. Nowicka, S. P. Davies, J. K. Edwards, C. D'Agostino, D. P. Mascarenhas, L. Durham, M. Sankar, D. W. Knight, L. F. Gladden, S. H. Taylor and G. J. Hutchings, *J. Phys. Chem. C*, 2011, **115**, 1073-1079.
41. F. Ganji, S. Vasheghani-Farahani and E. Vasheghani-Farahani, *Iran Polym J*, 2010, **19**, 375-398.
42. D. Danino, R. Gupta, J. Satyavolu and Y. Talmon, *Journal of colloid and interface science*, 2002, **249**, 180-186.
43. C. Wu and C.-Y. Yan, *Macromolecules*, 1994, **27**, 4516-4520.
44. W. F. J. Slijkerman and J. P. Hofman, *Magnetic Resonance Imaging*, 1998, **16**, 541-544.
45. I. Foley, S. A. Farooqui and R. L. Kleinberg, *J. Magn. Reson. Ser. A*, 1996, **123**, 95-104.
46. C. D'Agostino, M. R. Feaviour, G. L. Brett, J. Mitchell, A. P. E. York, G. J. Hutchings, M. D. Mantle and L. F. Gladden, *Catalysis Science & Technology*, 2016, **6**, 7896-7901.
47. C. D'Agostino, J. Mitchell, M. D. Mantle and L. F. Gladden, *Chemistry - A European Journal*, 2014, **20**, 13009-13015.
48. S. M. Russell and G. Carta, *Industrial & engineering chemistry research*, 2005, **44**, 8213-8217.
49. M. Helminger, B. Wu, T. Kollmann, D. Benke, D. Schwahn, V. Pipich, D. Faivre, D. Zahn and H. Cölfen, *Advanced functional materials*, 2014, **24**, 3187-3196.
50. M. Djabourov, N. Bonnet, H. Kaplan, N. Favard, P. Favard, J. Lechaire and M. Maillard, *Journal de Physique II*, 1993, **3**, 611-624.

606 51. Z. Yang, Y. Hemar, L. Hilliou, E. P. Gilbert, D. J. McGillivray, M. A. Williams and S.
607 Chaieb, *Biomacromolecules*, 2015, **17**, 590-600.
608 52. M. A. da Silva, F. Bode, I. Grillo and C. c. A. Dreiss, *Biomacromolecules*, 2015, **16**,
609 1401-1409.

610